Article:

Kechidi, S orcid.org/0000-0002-4922-7877 and Iuorio, O orcid.org/0000-0003-0464-296X (2022) Numerical investigation into the performance of cold-formed steel framed shear walls with openings under in-plane lateral loads. Thin Walled Structures, 175. 109136. ISSN 0263-8231

https://doi.org/10.1016/j.tws.2022.109136

Numerical investigation into the performance of cold-formed steel framed shear walls with openings under in-plane lateral loads

Smail Kechidi[a,b] and Ornella Iuorio[a]

[a]*School of Civil Engineering, University of Leeds, Leeds, United Kingdom*
[b]*ilke Homes Ltd., Knaresborough, United Kingdom*

Corresponding author. Tel.: +44 113 343 6729
E-mail address: s.kechidi@leeds.ac.uk (Smail Kechidi), o.iuorio@leeds.ac.uk (Ornella Iuorio)

Abstract. *Recently, there has been a resurgence in the adoption of lightweight cold-formed steel (CFS) profiles as structural elements in low- to mid-rise modular construction. Typically, openings for doors and windows are ever-present in the front and rear elevations where shear walls find their optimal position to ensure lateral stability in CFS modular structures. These architectural design features translate into reduced areas for lateral load resistance throughout the structure. This paper discusses the performance of CFS framed shear walls with openings under lateral loads through experimental tests and numerical simulations. Overall, three shear wall typologies were designed for force transfer around opening (FTAO) and tested under monotonic lateral loads (nine tests in total). An advanced finite element analysis (FEA) modelling protocol was elaborated to simulate the lateral behaviour of the tested walls as well as to interpret the physical tests. Evaluation of the numerical and experimental test results validated the FEA modelling protocol that demonstrated to be reliable in predicting the strength and stiffness as well as failure modes of CFS framed shear walls with openings subjected to lateral loads. The effects of sheathing-to-CFS screw spacing, the size and number of openings as well as the geometry of sheathing panels on the lateral behaviour of CFS framed shear walls were scrutinized. Subsequently, load-path mappings from the developed modelling protocol enabled the analysis of the flow of the in-plane lateral loads from the sheathing-to-CFS screw level into the wall system level where insight into a more efficient lateral design of CFS framed shear walls with openings have been highlighted. The obtained results shed light on the conservative nature of the AISI S400-15 design provisions for Type II shear walls and that of the perforated design methods available in the literature.*

Keywords: *Cold-formed steel; Perforated shear walls; Quasi-static monotonic tests; Nonlinear FEA; Lateral behaviour.*

1. Introduction

Cold-formed steel (CFS) framed shear wall is a subsystem that secures lateral stability in lightweight steel structures and is typically composed of studs, tracks, and blockings to which wooden structural panels (such as oriented strand boards - OSB) are screw-fastened to give rise to in-plane lateral strength and stiffness. As CFS profiles are generally made of slender cross-sections (Class 4 according to the classification of EN 1993-1-1 standard [1], usually referred to as Eurocode 3), the effective width method can be used to evaluate their axial and flexural design strengths in order to take into account the reduction resulting from local buckling effects [2]. Therefore, practicing engineers are referred to Parts 1-3, 1-5 and 1-8 [3-5] of Eurocode 3 (EC3) for, respectively, the design of CFS members and sheeting, plated structural elements, and joints. However, the current European code does not provide any guidance on the shear strength and stiffness provided by the sheathing-to-CFS screw fasteners in the above-described wall system which hinders its adoption in the UK and Europe. Consequently, design assisted by experimental tests and/or advanced finite element analysis (FEA) is recommended in such situations. In addition, details for force transfer around openings (FTAO) design have not yet been studied for CFS framed shear walls, therefore, advanced computational models along with experimental tests are deemed necessary for the proposal and assessment of efficient FTAO details that are tailored to CFS framed shear walls.

Over the last three decades, the behaviour of CFS framed shear walls has been examined experimentally and numerically under lateral and simultaneously lateral and vertical loads.

In particular a large number of experimental programs have been carried out to develop seismic design guidelines for CFS framed shear walls sheathed with wood-based panels, steel sheeting and gypsum panels, mostly without openings, in Canada (Branston et al. (2006) [6]), in the US (Serrette and Nolan (2009) [7]) and in Europe (Landolfo et al. (2006) [8]). Some researchers have studied the behaviour of CFS framed shear walls under both horizontal and vertical loads (Hikita and Rogers (2007) [9], DaBreo et al. (2014) [10], Iuorio et al. (2014) [11]) where, in particular, Hikita and Rogers (2007) [12] concluded that the effect of gravity loads, on the lateral performance of wood-sheathed CFS framed shear walls, is not detrimental provided that the chord studs are adequately designed. DaBreo et al. (2014) [10] established a comprehensive database of information, for steel-sheathed CFS framed shear walls, for Canadian design standards. Iuorio et al. (2014) [11] characterised the behaviour of bespoke wood-sheathed braced walls, and main wall components (OSB panels, connections and hold-downs) adopted for the first CFS building built in Italy, and confirmed the validity of adopting design capacities criteria for shear walls under lateral and gravity loads. Selvaraj and Madhavan (2019-2020) [12-13] investigated the effect of sheathing boards, C-section size and screw fastener types on the torsional buckling restraint of CFS studs wall under compression. Selvaraj and Madhavan (2019, 2021) [14-15]) studied the additional contribution that can be provided by gypsum based panels, and concluded that gypsum boards have insignificant contribution to bracing CFS studs, thus, should not be considered for design. Kyprianou et al. (2021) [16] experimentally studied gypsum-sheathed CFS wall studs under both compression and major axis bending. It was concluded that the failure mode for specimens sheathed with plasterboards is screw spacing dependent where a reduction from 600 mm to 75 mm resulted in a 30% increase in capacity. Some authors have investigated the shear wall behaviour for walls having a variety of height-to-width aspect ratio. In particular, Cheng Yu (2010) [17] determined the shear strength values of steel-sheathed CFS framed shear walls for different height-to-width aspect ratios. Based on experimental tests on 1.83 m wide and 2.44 m high steel-sheathed CFS framed shear walls, Yu and Chen (2011) [18] concluded that the shear strengths codified in AISI S213-07 [19] can conservatively be used for shear walls with an height-to-width aspect ratio equal to 3:2. Iuorio et al. (2012) [20] scrutinised the influence of the height-to-width aspect ratio on the lateral behaviour of CFS framed shear walls through code-based, analytical and numerical methodologies where similar values of strength and stiffness were obtained for shear walls with aspect ratios equal to 1:1 and 2:1. As far as the full structure behaviour is concerned, Landolfo et al. (2018) [21] has conducted shear wall tests on gypsum sheathed shear walls as well as shake table tests on two-storey CFS modular house, and assessed the additional contribution that nonstructural elements provide to the performance of the overall structural system in terms of dynamic properties (fundamental period of vibration and damping ratio), inter-storey drift and damage.

In parallel to experimental studies, numerical models have been established to predict the behaviour of sheathed CFS walls under a variety of loading conditions. Among those, Martínez-Martínez and Xu (2010) [22] proposed a numerical modelling technique for CFS framed shear walls which consists of an equivalent plate element whose physical and mechanical characteristics are determined taking into account the anisotropy of the wall and a constitutive model that takes into account the stiffness deterioration. Shamim et al. (2013) [23] used OpenSees to develop numerical models that simulate the two storeys shear walls. The numerical results highlighted the need to develop models that take into account the nonlinear behaviour of the shear walls as well as the elastic stiffness of the hold-downs so that the behaviour of the shear walls would be replicated with an acceptable accuracy. Nithyadharan and Kalyanaraman (2013) [24] used the Bouc-Wen-Baber-Noori (BWBN) model to simulate strength and stiffness deterioration as well as the pinch effect observed in CFS shear walls hysteretic loops. Buonopane et al. (2015) [25] elaborated a computationally efficient modelling protocol in OpenSees using beam-column elements to model the CFS frame and radial springs to model the OSB-to-CFS screw fasteners. Ye et al. (2016) [26] developed a simplified numerical model that reproduced with good degree of accuracy the test results obtained by Peterman and Schafer (2014) [27] in terms of axial load capacity and failure mode. Kechidi and Bourahla (2016) [28] developed and implemented two hysteretic models in OpenSees that take into account strength and stiffness deterioration with pinching effect observed in the lateral behaviour of steel- and wood-sheathed CFS framed shear walls. Kechidi et al. (2020) [29] developed a 3D modelling protocol for numerical parametric investigations of built-up back-to-back CFS channels under axial compression with the purpose of improving available design guidelines for chord studs in CFS shear walls. Deverni et al. (2020-2021) [30-31] simulated the lateral behaviour of OSB- and CP-sheathed CFS framed shear walls in ABAQUS where an acceptable accuracy of replicating the shear wall lateral behaviour has been obtained. Nithyadharan and Kalyanaraman (2021) [32] implemented the BWBN constitutive model in ABAQUS using a variably oriented spring pair element as a user-element (UEL) to model the cyclic behaviour of sheathing-to-CFS screw fasteners in CFS framed shear walls.

All tests and numerical models have highlighted the significant contribution played by CFS-to-sheathing connections.

Failure of the sheathing-to-CFS screw fasteners in an adequately designed CFS framed shear wall is usually assured via capacity-based design to prevent buckling of the chord studs. Based on this principles, design procedures for CFS shear wall frames have been proposed in [33-34]. In terms of walls with openings, which is the main subject of this paper, the lateral resistance capacity of long CFS framed shear walls with openings, the first tests were carried at the National Association of Home Builders (NAHB) research centre (1997) [35]. From the results of these tests, it was concluded that CFS framed shear walls exhibit a lateral resistance mechanism similar to that of timber-framed shear walls and the use of hold-downs decreases the wall uplift and improves its lateral resistance capacity. In addition, it was found out that the values of the shear strength of CFS framed shear walls with openings calculated using the empirical equation given by Sugiyama and Matsumoto (1994) [36] are reliable. Besides, a method for designing CFS framed shear walls with openings based on the same theory developed for timber-framed shear walls was recommended. Salenikovich et al. (2000) [37] tested CFS framed shear walls with and without openings under monotonic and cyclic loads where it was concluded that solid walls were stronger and stiffer, however, less ductile than perforated walls. Similar conclusions were drawn by Dolan and Easterling (2000) [38-39]; in addition, in monotonic tests, plasterboards brought 30% to the strength and stiffness of completely sheathed walls. By setting hold-downs at each end of the wall specimens, the semi-analytical approach gave conservative predictions. A total of 15 testes on CFS framed shear walls with two types of sheathings (corrugated steel sheets and OSB) as well as with X strap braces were performed by Fülöp and Dubina (2004) [40]. The walls were tested under cyclic and monotonic loads. By comparing the performance of the different tested walls, it was found out that the shear walls with plasterboards on their inner face experienced an increase in peak strength of approximately 17%. Considering the shear walls with openings, 60% decrease in terms of elastic stiffness and 20% to 30% decrease in terms of peak strength were endured. Based on a statistical analysis, Yang J. (2011) [41] proposed a design equation, in an exponential form, for CFS framed shear walls with openings.

Although the behaviour of CFS framed shear walls has significantly been studied under in-plane lateral loads and, to a lesser extent, with the consideration of door and window openings, no advanced computational models have been developed to serve as a virtual tests bench for the improvement and optimization of the lateral design of CFS framed shear walls with openings.

This paper aims to improve knowledge on the performance of CFS framed shear walls with openings under in-plane lateral loads by presenting numerical FEA investigations of walls with various configurations of openings size, number, and position that are validated based on a new experimental test campaign that has recently been undertaken. Specifically, the research study presented in this paper has mainly focused on the lateral performance of CFS framed shear walls with openings manufactured by ilke Homes Ltd. In the first instance, this involved the characterization of the CFS material properties as well as the sheathing-to-CFS screw shear behaviour. Afterwards, nine monotonic tests have been performed on three different shear wall typologies designed according to the FTAO method. An advanced FEA modelling protocol was elaborated to simulate the lateral behaviour of the tested walls as well as to interpret the physical tests. Comparison between numerical and experimental test results validated the FEA modelling protocol that turned out to be accurate in replicating the strength and stiffness as well as the failure modes of CFS framed shear wall with openings subjected to lateral loads. Subsequently, an assessment of the demand-to-capacity (DC) ratio, as well as the displacement vector diagram of the sheathing-to-CFS screws at various levels of lateral displacement, disclosed the flow of the in-plane lateral loads from the sheathing-to-CFS screw level into the wall system level. Finally, a comparison of FEA and experimental test results is made with estimates of strength using the AISI S400-15 [42] design provisions for Type II shear walls and that of the perforated design methods available in the literature.

2. Experimental testing

As part of the experimental testing program of this study, tensile tests on CFS coupons and shear tests on sheathing-to-CFS screw fasteners have been carried out with the aim of acquiring information necessary for the lateral design of CFS framed shear walls and elaborating their FEA models. In addition, nine monotonic tests on three different shear wall typologies under in-plane lateral loads have been completed.

It is worth mentioning that although several tests have been carried out on different sheathing boards (*e.g.*, Ornella Iuorio (2009) [43] and Kyprianou et al. (2021) [44]), conservative assumptions were made herein for OSB and cement particle (CP) boards by adopting values of the material properties given by the manufacturer which coincide with the minimum recommended by BS EN 12369-1 (2001) [45].

2.1. Coupon testing for CFS characterization

In accordance with BS EN ISO 6892-1 (2019) [46], 16 tensile tests were carried out on coupons cut longitudinally from C100-41-1.6, C100-65-1.6, C150-65-1.6 and C200-65-2.0 profiles that form the frame of the specimens described in Sections 2.2 and 2.3. As shown in Figure 1, two coupons from the web and one coupon from each flange were taken from each profile. The BS EN ISO-dictated coupon dimensions are shown in Figure 2. For each set of coupons, mean values of the uncoated thickness, yield strength, tensile strength, as well as the strain at tensile strength and fracture are listed in Table 1. For the measurement of the uncoated thickness, the zinc coating was removed from both ends of all coupons using 1M HCl solution. All yield strength mean values are above the nominal 450 MPa except for the coupons cut from C100-65-1.6 and C150-65-1.6 profiles. As all the tested coupons are of the same steel grade (S450), the weakest tensile test results were opted for to model the CFS material in Section 3 in order to be on a conservative side rather than on a permissive one.

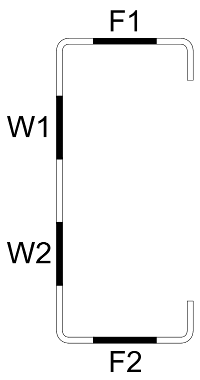

Figure 1. Position of coupons in C-shaped cross-section [47].

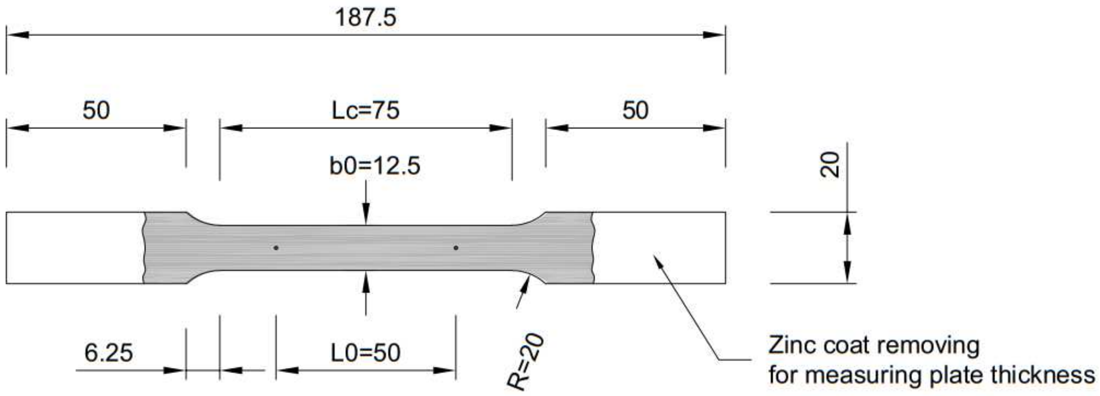

Figure 2. CFS coupon dimensions (unit: mm) [47].

Table 1. Tensile test results.

Section	Uncoated thickness t (mm)	Length elongation ΔL_g (%)	Yield strength[a] $F_{y,0.2}$ (MPa)	Yield strength[b] $F_{y,\,auto}$ (MPa)	Upper yield strength $F_{y,\,upper}$ (MPa)	Young's Modulus (MPa)	Tensile strength F_u (MPa)	Strain at tensile strength ε_u (mm/mm)	Strain at fracture ε_r (mm/mm)
C100-41-1.6	1.56	11.67	472.40	472.03	472.73	216130	495.45	0.07	>0.10
C100-65-1.6	1.75	21.79	441.08	443.50	446.88	212415	521.40	0.13	>0.17
C150-65-1.6	1.57	9.34	413.20	426.13	423.23	235020	446.13	0.05	>0.09
C200-65-2.0	2.06	22.37	471.65	494.43	488.38	205050	549.03	0.12	>0.17

[a]*Yield strength at 0.2% offset;*
[b]*Yield strength at the average of 0.4% and 0.8% offsets.*

2.2. Sheathing-to-CFS screw shear tests

In CFS framed shear walls, the lateral stability is mainly ensured by the shear strength and stiffness provided by the sheathing-to-CFS screws as a result of the incompatibility between the deformed shape of the CFS frame (parallelogram) and that of the sheathing (rigid rotation) [25]. As shown in Figure 3, the screw tilts and bears against the sheathing then pulls through until failure is reached; this is the typical sequence of damages in an appropriately designed CFS framed shear wall subjected to increasing lateral loads. This sequence of damages is conditional on applying a capacity design approach and meeting the minimum allowable distance requirement between the longitudinal axis of the screw and the sheathing edge (see Figure 3) which is highly dependent on the sheathing material and thickness. Therefore, in order to investigate the effects of the sheathing type and thickness as well as the distance between the screw longitudinal axis and the edge of the sheathing (*i.e.*, the edge distance) on the shear behaviour of sheathing-to-CFS screw fasteners, a total of twelve tests have been performed on OSB- and CP-to-CFS screw fasteners.

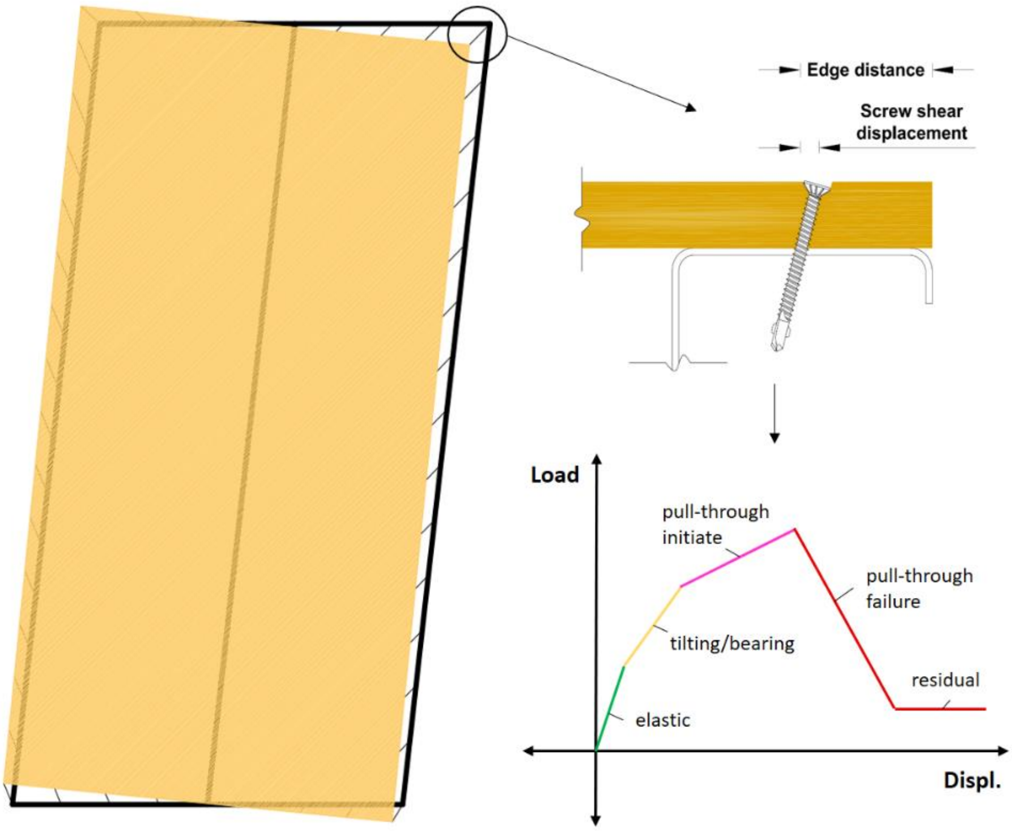

Figure 3. Typical deformed shape of CFS framed shear wall subjected to in-plane lateral loads (left), and resulting shear displacement on CFS-to-sheathing screw along with its performance (right).

Figure 4 depicts the results in terms of shear load vs. displacement of OSB- and CP-to-CFS assembly for 10.25 mm and 20.5 mm edge distances. It can be noticed that the curves are comparable with an acceptable variation. From a failure-mode perspective, the specimens endured five different performance stages. The first stage (up to 40% of peak load) represents the elastic extent where the screws started to tilt without any damage to the sheathing. In the second stage (up to 80% of the peak load), some sheathing damages arose which is mainly caused by the bearing of screws against the sheathing. In the third stage (up to 100% of the peak load), the screws started to pull through the sheathing and further deterioration of the shear stiffness occurred until the peak load was reached. The post-peak stage took place after the head of the screws has penetrated significantly through the depth of the sheathing; the shear load started deteriorating until reaching the final stage where a residual load of the assembly was observed up to the largest tested displacement.

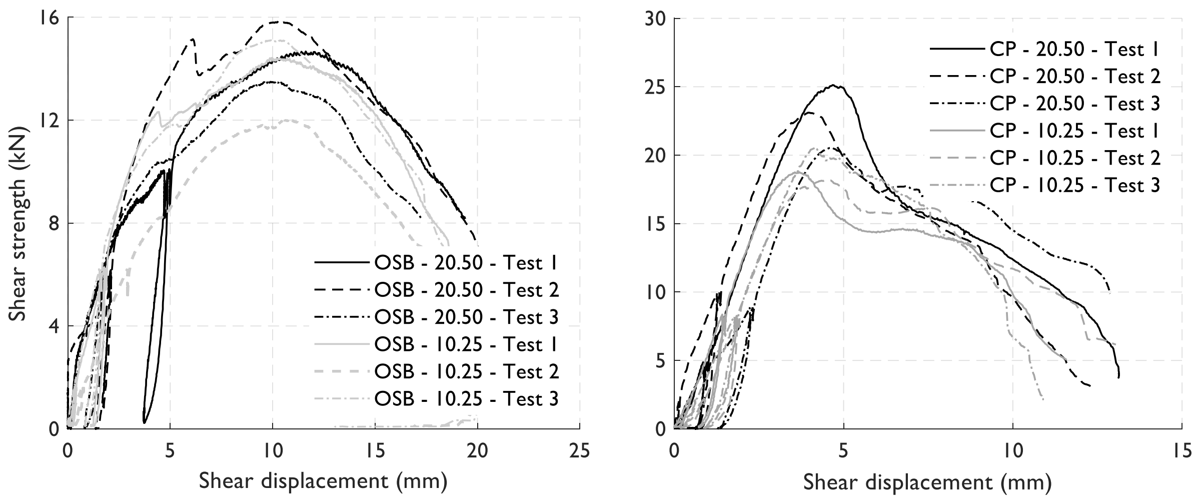

a) b)

Figure 4. Load vs. displacement curves for: a) OSB- and b) CP-sheathed specimens [47].

2.3. CFS framed shear wall design and testing

Two methods are available for the design of CFS framed shear walls with openings to resist in-plane lateral loads. The segmented method represents the traditional design approach where only full-height segments are considered, the contribution of sheathing above and below openings is ignored, and hold-downs are typically required at each end of the full-height segments to resist overturning forces. On the other hand, the perforated method accounts for openings using empirical adjustment factor based on the percentage of full-height wall segments adjacent to openings and hold-downs are only required at each end of the total wall length without any details for force transfer around openings. The FTAO method, instead, is a favoured design approach for timber-framed shear walls which allows for utilization of the full wall geometry including sheathed areas above and below openings. In this method, the sheathing-to-frame fasteners transfer the applied force, anchor bolts resist sliding force which is equal to the applied force divided by the total length of the wall and hold-downs are only required at each end of the total wall length to resist overturning forces. Strengthening around openings is normally accomplished by increasing fasteners around the corners of the openings, adding blocking and/or strapping in order to transfer force around openings effectively. Given the similarity between timber and CFS framed shear walls in terms of lateral resistance mechanism, the FTAO method has been adopted herein for the lateral design of CFS framed shear walls with openings.

In this section, the description and design of shear wall specimens as well as the basic summary of the test results are provided. A total of three CFS framed shear wall typologies with various configurations of door and window openings were designed according to the FTAO method. As such, the designed shear walls have a reduced number of hold-downs reflecting the typical external walls in the front and rear elevations of ilke Homes ground- and upper-floor modules. Shear wall frames are pre-assembled from lipped channel C100-41-1.6 (nominal sizes: 100 mm (web) x 41 mm (flange) x 11 mm (lip) x 1.6 mm (thickness)) CFS studs with a nominal grade of 450 MPa typically spaced at 600 mm centres. Multiple stud configurations are arranged into back-to-back built-up cross-sections around the openings and are fastened with two self-drilling hex washer head screws vertically at 400 mm centres. At the OSB joints, lipped channel size C100-65-1.6 (100 mm x 65 mm x 13 mm x 1.6 mm) is used instead to allow for a larger distance between the screw longitudinal axis and the edge of the sheathing. C200-65-2.0 (200 mm x 65 mm x 13 mm x 2 mm) and C150-65-1.6 (150 mm x 65 mm x 13 mm x 1.6 mm) ledger tracks of, respectively, floor and ceiling cassettes are fixed into the inner face of the walls with two hex washer head screws (self-drilling) per stud position. Only one side of the wall is sheathed with 15 mm thick OSB. The geometry of OSB panels is schematised in table 2. 12.5 mm thick CP boards are used as water resistant sheathing for the ground floor wall from the base up to 300 mm high (see Figure 5). Steel-to-steel flat pancake head screws were used to connect the studs to top and bottom tracks and the studs to blockings. Self-drilling star head screws are used for fastening all sheathing boards to the frame. Screw spacing centres in the different areas of the walls are shown in Figure 5. M12 bolts of grade 8.8 are used to attach two C100-41-1.6 studs to build up the chord studs. Simpson Strong-Tie HTT22E hold-down is installed in each bottom corner of the walls using 31 steel-to-steel screws. The walls are connected to the top and bottom steel beams of the test setup via M16 anchor bolts where their positions are shown in Figure 5.

The individual cross-sections of the shear walls are all load bearing and as such are all designed to resist dead, live, and wind loads. Sheathing-to-CFS screw density is design in such a way as to be under the takt time of an automated high-speed panel line (HSPL) - 600 screws per cycle for one pair of walls. The walls are designed to cover 80% of England considering wind speed velocity, distance to shore, and altitude above sea level. The sheathing layout was designed to have the least possible cuts through the adoption of off-the-shelf OSB panels, to significantly reduce material waste while keeping the code-allowable height-to-width aspect ratio (*i.e.*, 4:1 according to AISI S400-15 [42]) of each full-height segment of the wall. C-shaped sheathing panels have been purposely designed for force transfer around openings (see schematic views in Table 2).

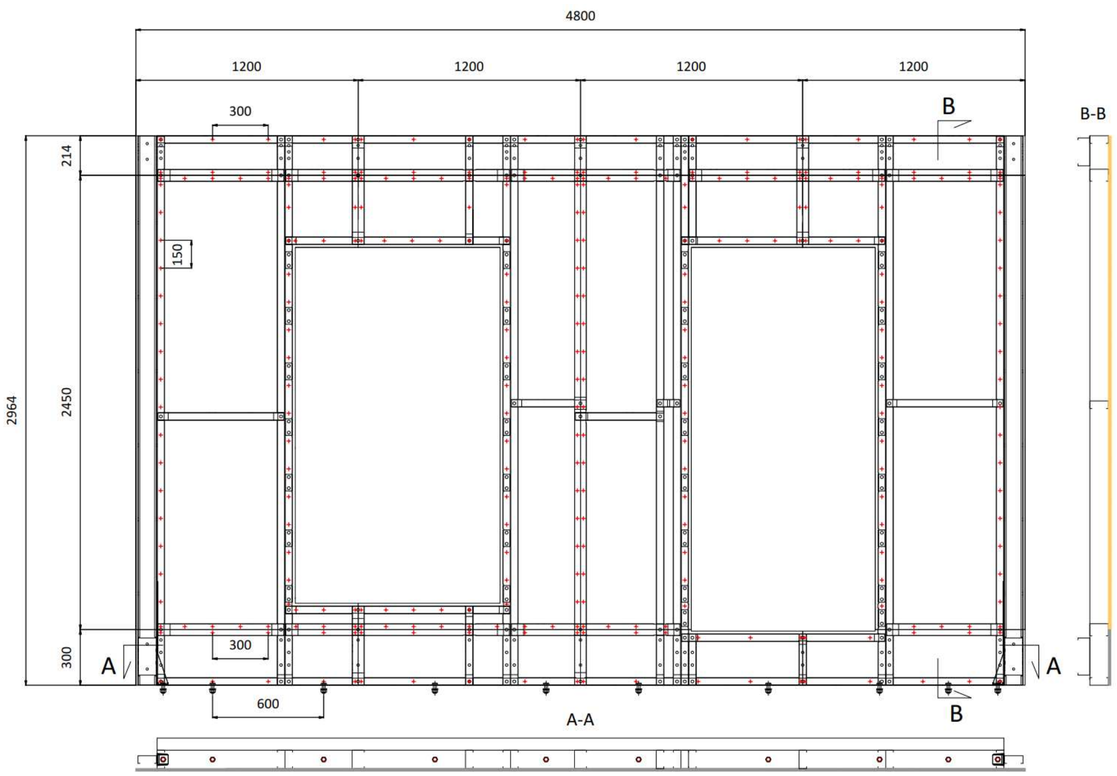

a)

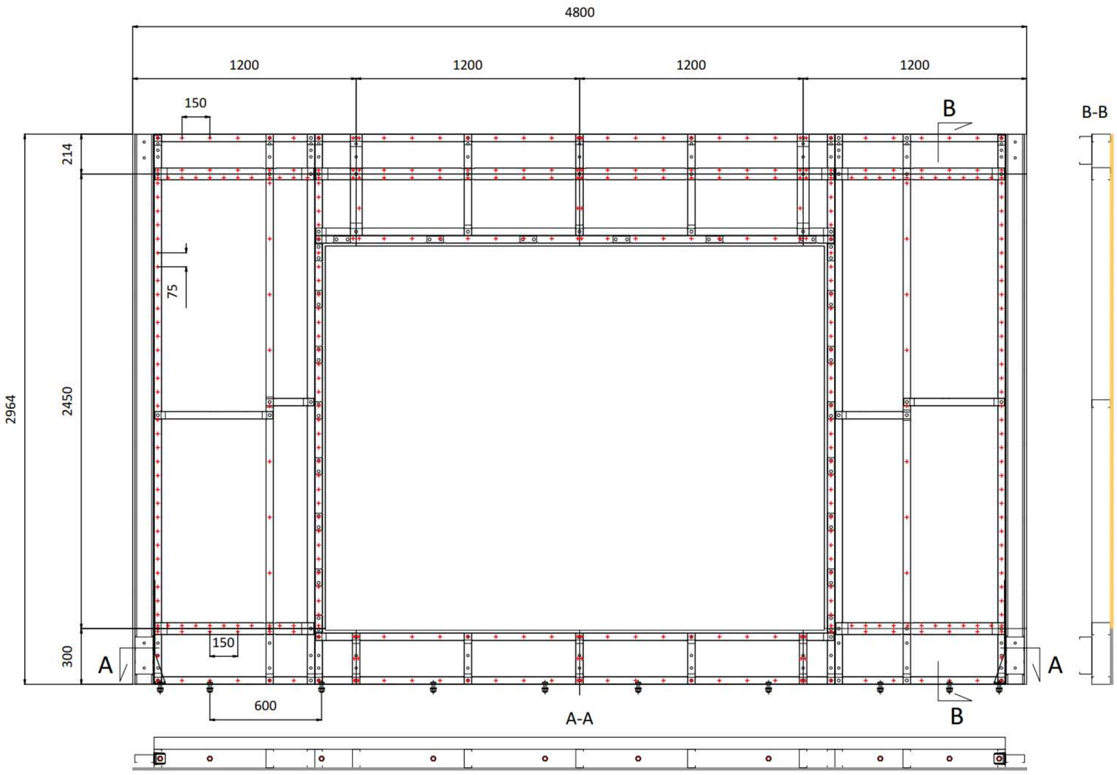

b)

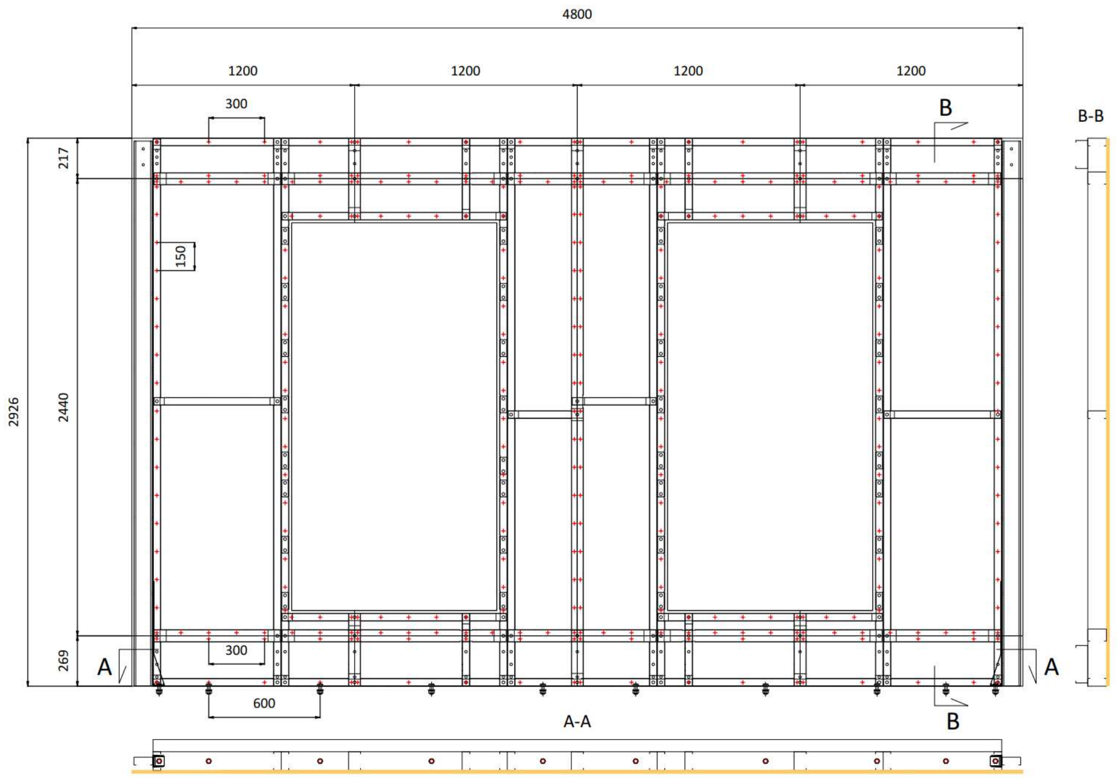

c)

Figure 5. Shear wall configuration: a) ground-floor front wall (GF-FW), b) ground-floor rear wall (GF-RW) and c) first-floor front and rear wall (FF-F&RW).

Three tests were carried out on each wall typology in accordance with BS EN 594: 1996 [48] where the applied loading protocol is shown in Figure 6. The test setup shown in Figure 7 was developed according to the same standard.

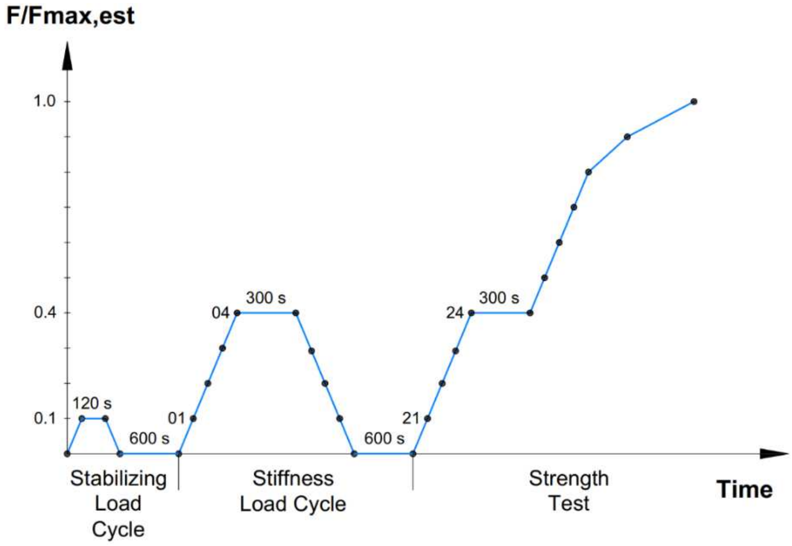

Figure 6. BS EN 594 loading protocol [48].

Figure 7. Test setup.

The test results of the above-described shear walls are listed in Table 2. The lateral stiffness was calculated according to Section 6.5 of BS EN 594:1996 [48].

Table 2. Shear wall test results.

Wall configuration	**Test number**	**Height x width (mm)**	**Screw spacing*** **(mm)**	**Peak lateral load (kN)**	**Stiffness (kN/mm)**	**Failure mode**
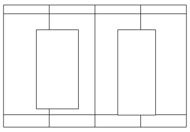	1	2964 x 4800	150/300	55.62	2.02	Opening corner cracks
	2			61.40	2.49	Opening corner cracks
	3			61.61	2.54	Opening corner cracks
	Mean			**59.54**	**2.52**	-
	STDEV			**2.78**	**0.23**	-
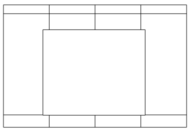	1	2964 x 4800	75/150	64.30	1.79	Opening corner cracks
	2			64.90	1.71	Opening corner cracks
	3			58.00	1.95	Opening corner cracks
	Mean			**62.40**	**1.82**	-
	STDEV			**3.12**	**0.10**	-
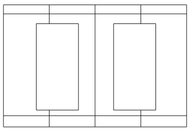	1	2926 x 4800	150/300	58.68	1.70	Opening corner cracks
	2			59.70	1.87	Opening corner cracks
	3			60.14	1.94	Opening corner cracks
	Mean			**59.51**	**1.91**	-
	STDEV			**0.61**	**0.10**	-

**Screw spacing in the middle part of the wall (either 150 mm or 75 mm)/the screw spacing at the top and bottom stripes of the wall (either 300 mm or 150 mm).*

3. FEA modelling of CFS framed shear walls

In order to develop advanced computational models of the tested CFS framed shear walls that provide reliable results with a reasonable computational cost, a 3D FEA modelling protocol has been developed in ABAQUS/CAE (2017) [49]. Figure 8 shows the meshed components of the GF-FW shear wall.

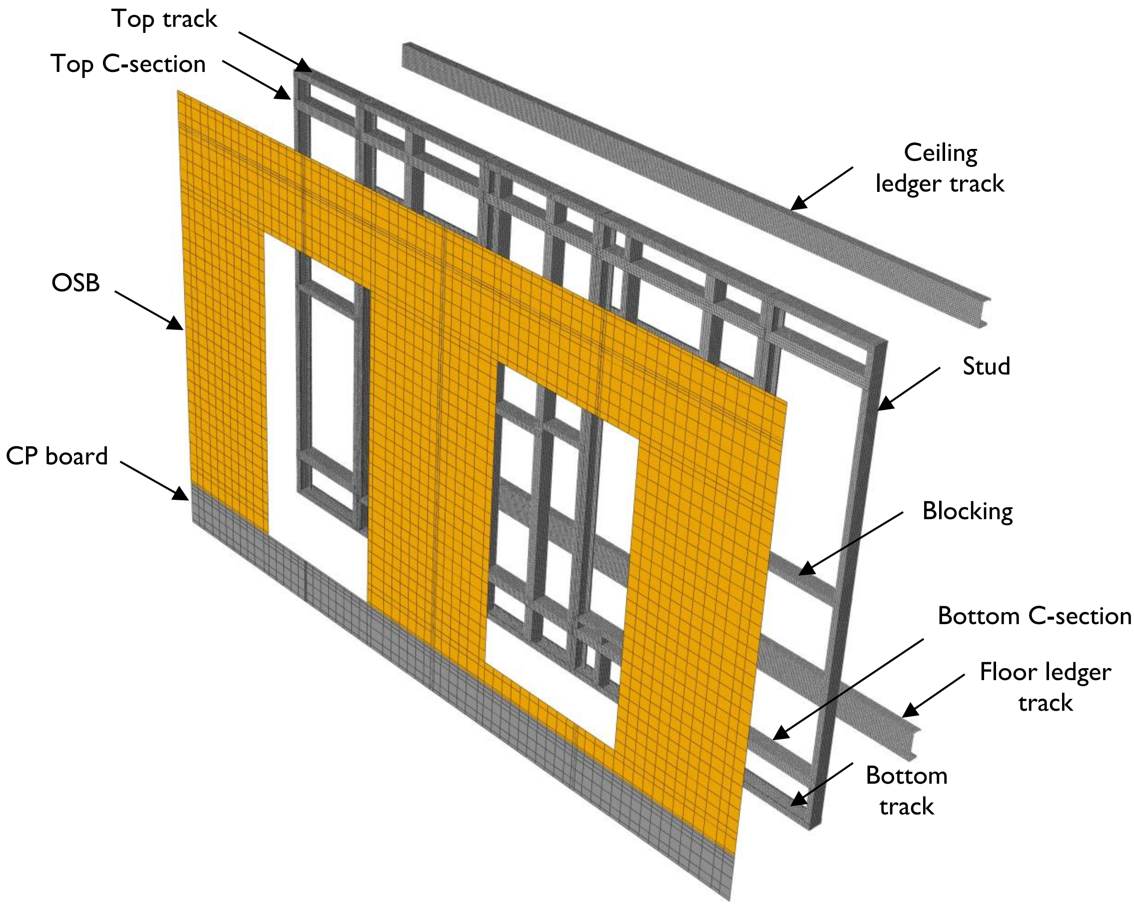

Figure 8. Exploded view of the GF-FW shear wall model.

3.1. Element and material modelling of CFS

The studs, tracks, blockings, and ledger tracks were modelled with 9-node doubly curved thin shell elements, reduced integration, using five degrees of freedom per node known as S9R5 [49]. As depicted in Figure 8, a fine mesh was used for these framing elements which are discretized at every 10 mm along the longitudinal axis of their cross-section with an aspect ratio approximately equal to 1:1. In terms of material model, the classical von Mises plasticity with isotropic hardening was chosen [29]. The Young's modulus was assumed to equal 210 GPa and the Poisson's ratio was taken as 0.3. The plasticity was modelled by indicating the true stress and true plastic strain (see Figure 9) obtained from the tensile tests described in Section 2.1.

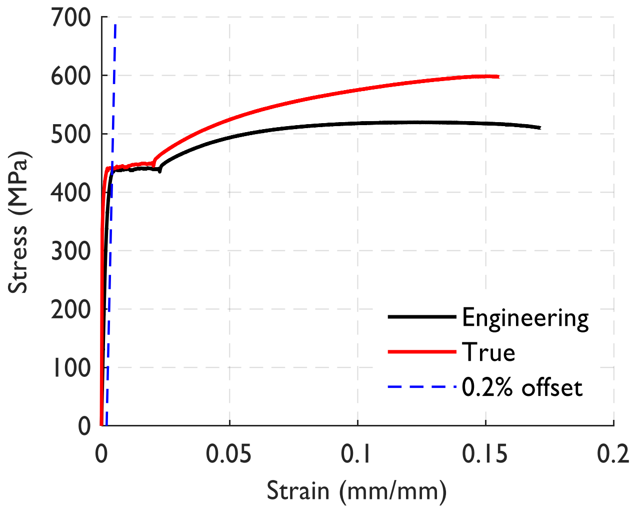

Figure 9. Tensile test results of C100-41-1.6-F2 coupon [47].

In this study, yield and tensile strength enhancements in the corner regions of the framing elements due to cold forming were not considered in the FEA models, as their effect on the lateral behaviour (initial stiffness, peak strength and failure mode) of the simulated shear walls is insignificant. This is mainly due to the small corner area compared to the total area of the cross-section of the framing elements, the presence of the sheathing boards and the small thickness of the cross-section, which leads to a moderate corner radius [50].

3.2. Element and material modelling of OSB and CP boards

The OSB and CP boards were modelled with 4-node general-purpose shell, reduced integration with hourglass control, finite membrane strains known as S4R [49]. A relatively coarse meshing was adopted for the sheathing where elements are discretized at 75 mm along their length with an aspect ratio approximately equal to 1:1 and never exceeding 2:1. Since the parallel and perpendicular material properties of OSB are different, an elastic orthotropic material model was used for the OSB. The orthotropic elasticity was defined by specifying the engineering constants *i.e.*, Young's modulus equal to 3800 MPa and 3000 MPa (parallel and perpendicular to span, respectively), Poisson's ratio was taken as 0.3, and the shear modulus in the principal directions equal to 1080 MPa [51]. An isotropic elastic material model, with the Young's and shear modulus equal to 9135 MPa and 3513 MPa, respectively, and the Poisson's ratio of 0.3 [52] was adopted to model the CP boards.

3.3. Element and material modelling of screws

In order to simulate the shear behaviour of the OSB- and CP-to-CFS screw-fastened connections in ABAQUS, user-defined element (UEL) subroutines were adopted to adequately capture the strength and stiffness deterioration observed and discussed in Section 2.2. These screws were modelled as radial springs with Pinching4 [53] constitutive model, initially implemented in OpenSees [54], that was integrated into ABAQUS through a Fortran script developed by Chu Ding (2015) [55].

Since the connections between the framing elements in CFS shear walls are considered pinned, the screws connecting studs to tracks, blockings, and ledger tracks were modelled by restraining all three translational degrees of freedom (DOF) of the nodes that coincide with the connection zone of stud-to-track/blocking/ledgers tracks using the linear constraint equation in ABAQUS [49] while releasing all three rotational DOF. The same approach was followed for modelling the screws that connect two C-sections to form back-to-back built-up jamb studs.

3.4. Boundary conditions and solution algorithm

As a stiff beam was connected to the top track via anchor bolts through which lateral forces were applied on the tested shear walls, displacement-controlled loading was enforced to the nodes that coincide with the anchor bolts position. The DOF corresponding to the out-of-plane displacement of these nodes was fixed. The loading was modelled by applying imposed longitudinal displacements at these nodes as shown in Figure 10. At the bottom track, the nodes coinciding with the shear anchors position were fixed in the horizontal directions as shown in Figure 10. As described in Section 2.3, at both ends of the tested shear walls, hold-downs are fastened to the web of the chord stud and anchored to the bottom track. The hold-downs were modelled by assigning a rigid body to tie the DOF of the nodes in the web of the chord stud that coincide with the contact area between the hold-down and the chord stud (representing the slave nodes) to the master node that is located in the center of gravity of that area (see Figure 10). Using Spring2 element, the master node is then fastened to the ground with a stiffness equal to 1000 N/mm in tension and 1000 times that value in compression as recommended by Buonopane et al. (2015) [25].

The nonlinear equilibrium equations were solved using the Newton-Raphson integration approach with artificial damping while geometric nonlinearity was taken into account. An artificial damping factor of 1.e-05 was opted to avoid overestimating the responses of the shear walls. The reason behind using artificial damping in the analyses is to ensure convergence at high lateral displacements. An output of the ALLSD/ALLIE (the energy dissipated by viscous damping to the total strain energy ratio) over the relevant total displacement was checked to make sure that the adopted damping factor has not been exceeded as per the guidance in the ABAQUS manual [49].

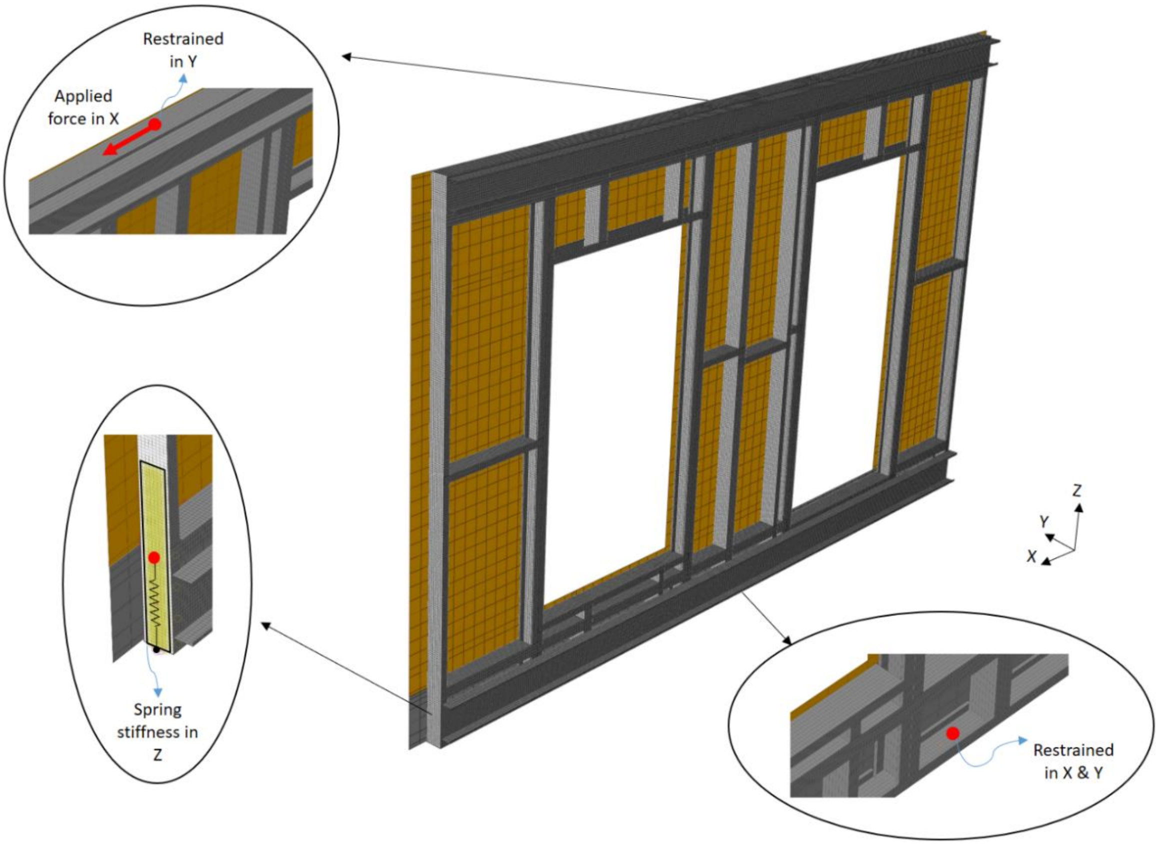

Figure 10. Modelled boundary conditions.

3.5. Validation of the proposed FEA modelling protocol

a) Load vs. displacement curves

Lateral load vs. displacement curves from monotonic tests on full-scale shear walls are plotted in Figure 11 together with the corresponding FEA results. Overall, the developed FEA modelling protocol simulates the lateral behaviour (strength and stiffness) of the tested shear walls with acceptable reliability throughout all levels of lateral displacement. The results illustrate that the peak lateral load of the tested shear walls is captured with a maximum difference of 4%, 4%, and 1% from, respectively, the mean of the three experimental peak lateral loads of the GF-FW, GF-RW, and FF-F&RW. The lateral displacement at peak load is accurately captured with 1%, 1%, and 2.5% difference from the mean of the three experimental peak lateral displacements at peak load of the GF-FW, GF-RW, and FF-F&RW, respectively. The above-described results are outlined in Table 3.

Although the screw spacing in the GF-FW (150/300 mm) is higher than in the GF-RW (75/150 mm), the initial stiffness is lower in the GF-RW (2.52 kN/mm vs. 1.82 kN/mm). This is mainly due to the large area of the door opening leading to a less effective force transfer around the openings, thus, resulting in a more flexible shear wall. However, similar values were obtained in terms of peak load. Comparing the performance of the GF-FW with that of the FF-F&RW, it can be noticed that the initial stiffness of the GF-FW is higher than that of the FF-F&RW (2.52 kN/mm vs. 1.91 kN/mm) despite the fact that the screws in both shear walls are fastened at the same spacing (*i.e.*, 150/300 mm). However, the main differences between the two shear walls are the location of the openings and the use of CP boards in the ground-floor wall. The height of the OSB in the GF-FW is 2450 mm and 2440 mm in the FF-F&RW which overcame the additional two corners in the FF-F&RW shear wall in terms of lateral strength contribution to the overall wall system.

The tested and simulated shear walls exhibit a ductile behaviour where the peak load is only reached when every sheathing-to-CFS screw fastener has yielded and this in turn led to lateral displacements at peak load of ~100 mm. It is worth noting that the sheathing-to-CFS screws were given the mean values of the results shown in Figure 4. A detailed analysis of the DC ratio and of the flow of the in-plane lateral loads from the sheathing-to-CFS screw level into the wall system level is presented in Section 4.

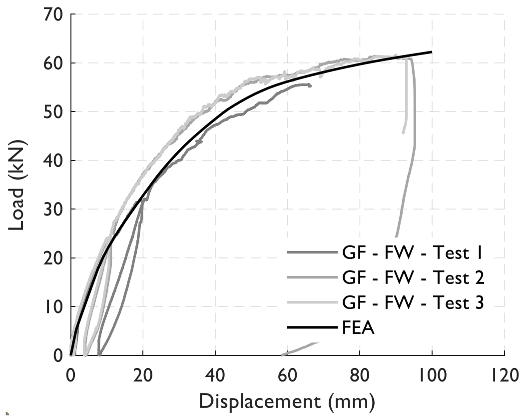

a)

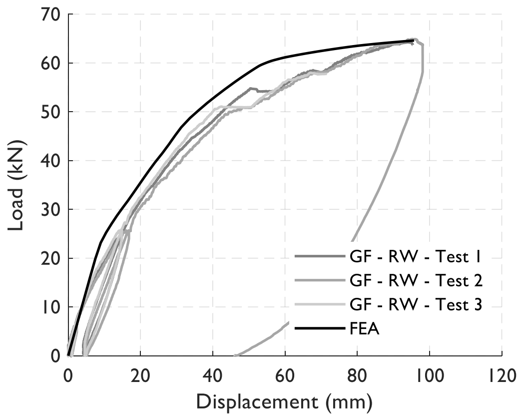

b)

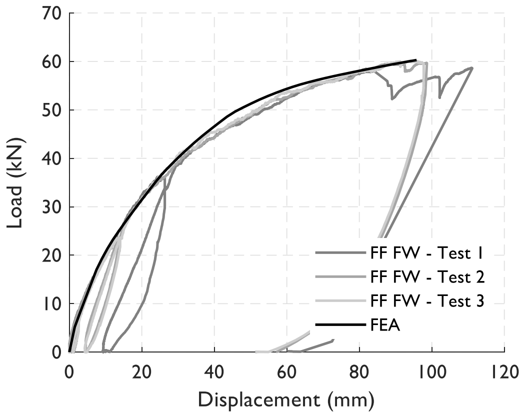

c)

Figure 11. Plots of measured and simulated lateral load vs. displacement for: a) GF-FW, b) GF-RW and c) FF-F&RW.

Table 3. Test and FEA results summary.

Wall configuration	Test number	Tests			FEA		
		Peak lateral load (kN)	Disp. @ peak lateral load (mm)	Stiffness (kN/mm)	Peak lateral load (kN)	Disp. @ peak lateral load (mm)	Stiffness (kN/mm)
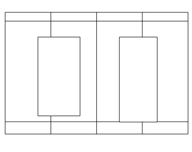	1	55.62	**-**	2.02	61.50	93.60	2.17
	2	61.40	**95.20**	2.49			
	3	61.61	**92.89**	2.54			
	Mean	**59.54**	**94.05**	**2.52**	**-**	-	-
	STDEV	**2.78**	**1.16**	**0.23**	**-**	-	-
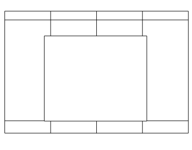	1	64.30	95.39	1.79	64.52	95.71	2.47
	2	64.90	98.10	1.71			
	3	58.00	-	1.95			
	Mean	**62.40**	**96.74**	**1.82**	**-**	-	-
	STDEV	**3.12**	**1.36**	**0.10**	**-**	-	-
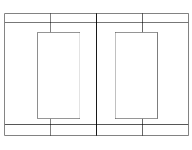	1	58.68	-	1.70	60.28	95.80	2.07
	2	59.70	98.65	1.87			
	3	60.14	97.76	1.94			
	Mean	**59.51**	**98.21**	**1.91**	**-**	-	-
	STDEV	**0.61**	**0.45**	**0.10**	**-**	-	-

b) Failure modes

Figures 12-14 show the failure modes in the tested and simulated GF-FW, GF-RW, and FF-F&RW shear walls at the peak lateral displacement. For all walls, the failure started with diagonal cracks in the OSB sheathing around the corners of the door and window openings at the onset of 50 mm lateral displacement. Cracks length and width kept increasing as the applied lateral force increases until the largest tested displacement (*i.e.*, ~ 100 mm) was reached where the OSB sheathing ended up with shearing. The above-described failure mode was mainly due to the fact that C-shaped sheathing boards tend to deform in a rigid rotation while ensuring the FTAO mechanism, thus, a high concentration of stresses took place around the corners of the door and window openings. A similar trend is obtained from the FEA simulations as shown in Figures 12a, 13a and 14a where a high-stress concentration around the corners of the door and window openings is observed in the Von Mises stress contours. Parts of the sheathing boards that are under stresses higher than their ultimate tensile strength which equals to 7.0 MPa are shown in grey.

The above-described failure mode, which is guaranteed by the FTAO design method, allowed for the shear forces applied on the sheathing-to-CFS screws to be redistributed in such a way as to yield all the connections before reaching the peak load of the shear walls. Further discussion on the shear demand on the sheathing-to-CFS screws is provided in Section 4. Overall, this failure mode is more desirable as it gives a better lateral performance of CFS framed shear walls with openings. A comparison with the results of perforated design methods in terms of peak lateral resistance is provided in Section 5.

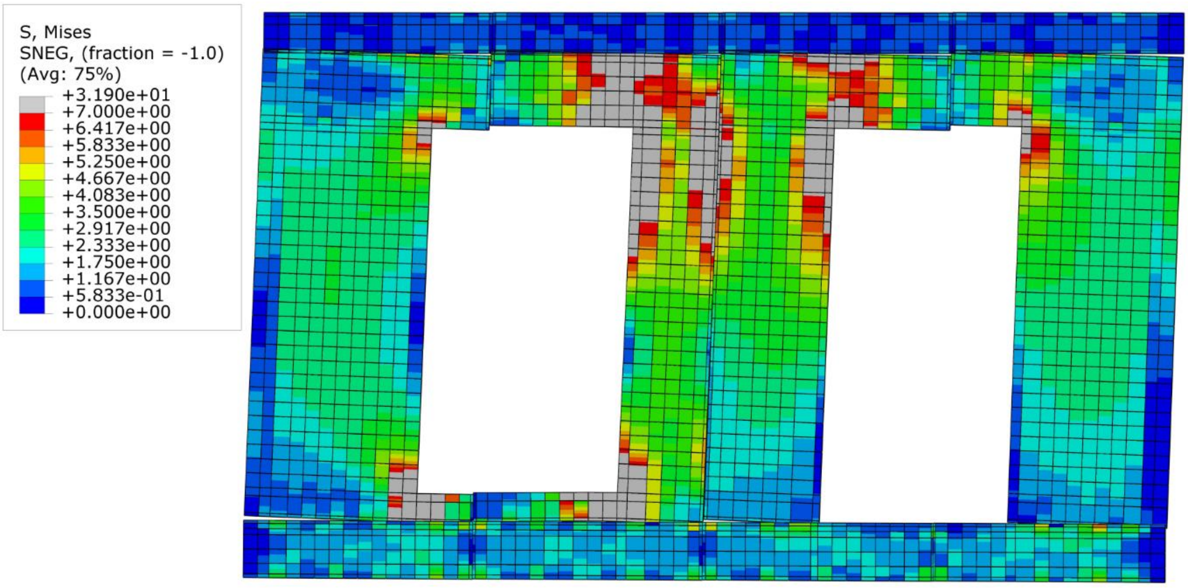

a)

b)

Figure 12. a) FEA simulated and b) measured deformations at peak load for GF-FW.

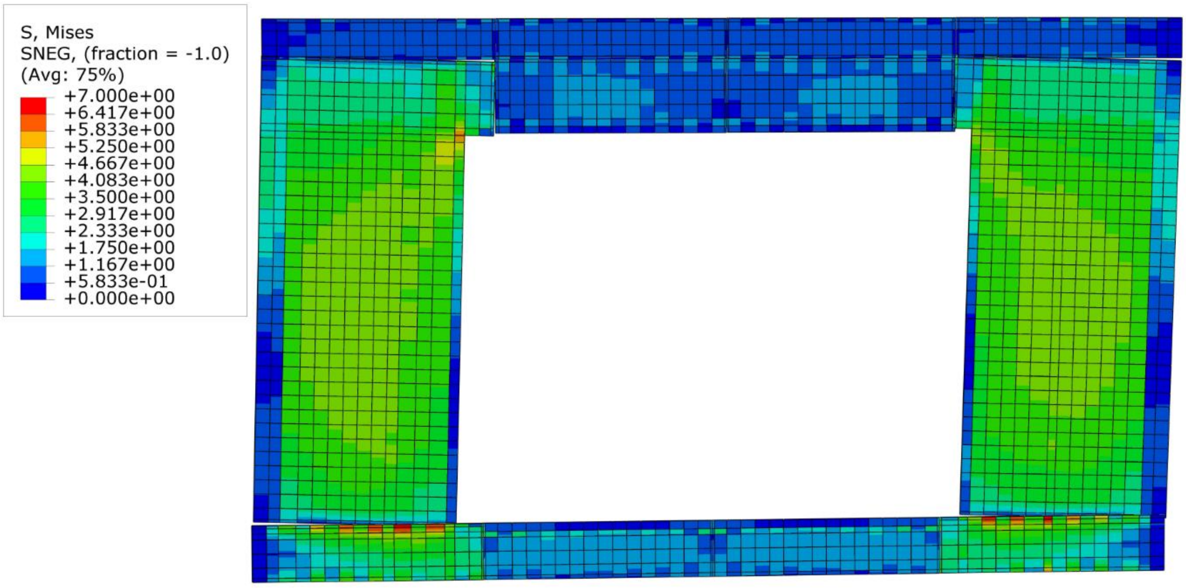

a)

b)

Figure 13. a) FEA simulated and b) measured deformations at peak load for GF-RW.

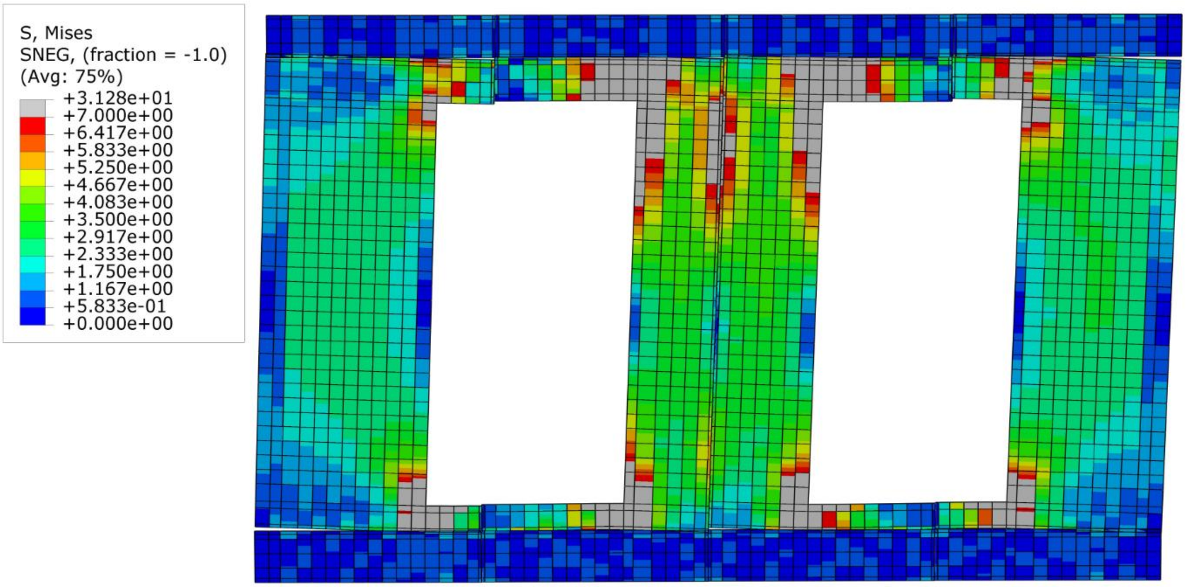

a)

b)

Figure 14. a) FEA simulated and b) measured deformations at peak load for FF-F&RW.

4. Shear wall load path mappings from FEA simulation

In this section, the developed FEA modelling protocol is employed to analyse the flow of the in-plane lateral loads from the sheathing-to-CFS screw level into the wall system level. As the sheathing-to-CFS screws carry the applied lateral forces, assessment of the shear force on these connections at peak load of the walls, shown in Figures 15-17, reveals that the screws at the vertical straight edges of the sheathing boards endure the largest forces. Screws in the top and bottom stripes of the shear walls are not capitalized in terms of lateral resistance contribution owing to the fact that the ceiling and floor ledger tracks generate a portal action that represents the main lateral resistance mechanism in these specific parts of the shear walls. The load paths follow classical assumptions where the screws fastening the perimeter of the sheathing boards in CFS framed shear walls experience higher shear demand compared to field screws (in the jamb studs) due to the rigid rotation of the boards under lateral loads. Accordingly, the screw density in the top and bottom stripes of the walls was designed as 50% lower by doubling the screw spacing. Furthermore, screws around the door and window openings endure high shear demand, as they are part of the FTAO detailing.

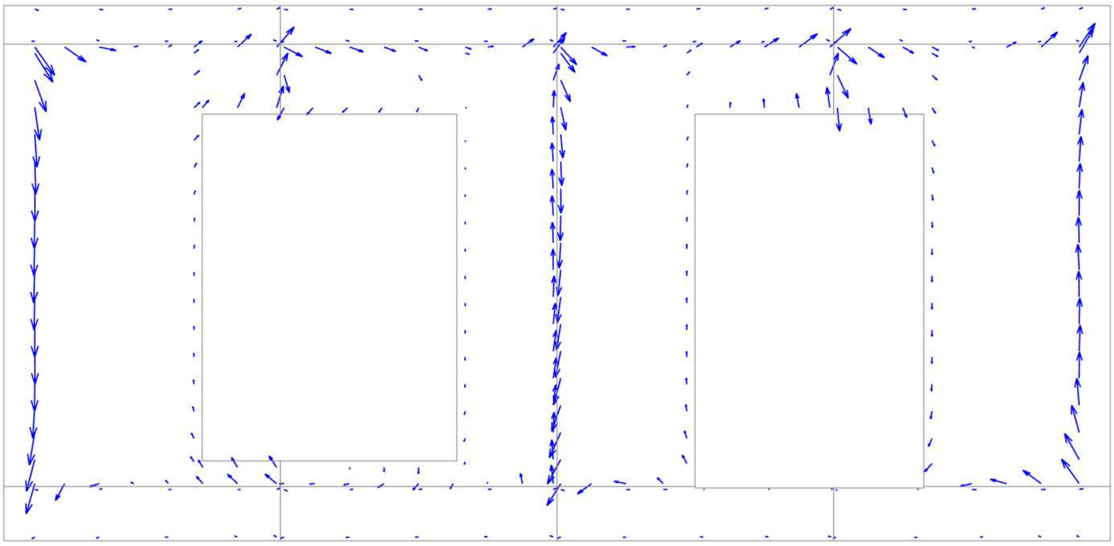

Figure 15. Screw demand capacity (DC) displacement vector diagram at peak lateral load for GF-FW model.

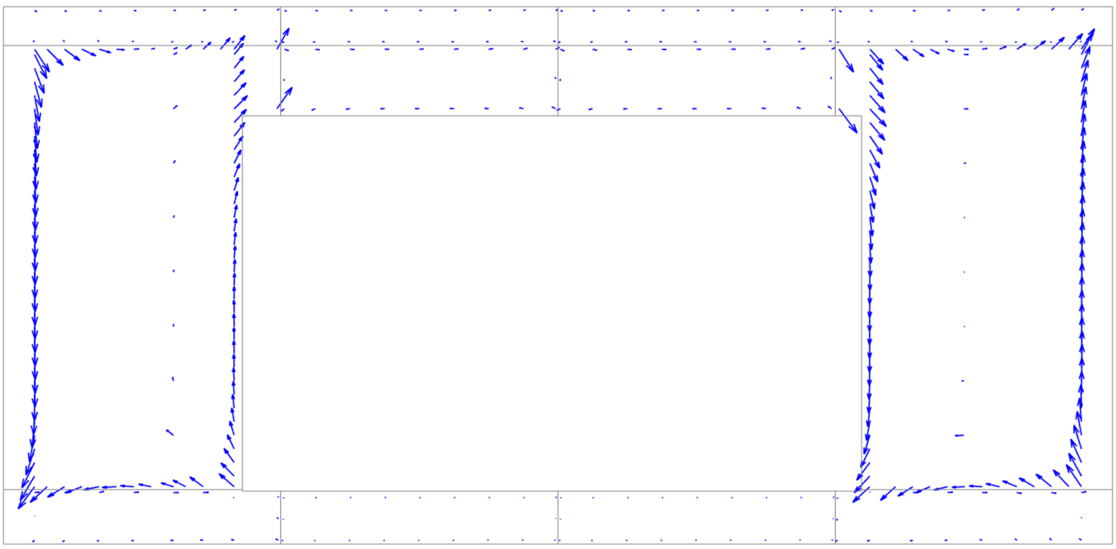

Figure 16. Screw DC displacement vector diagram at peak lateral load for GF-RW model.

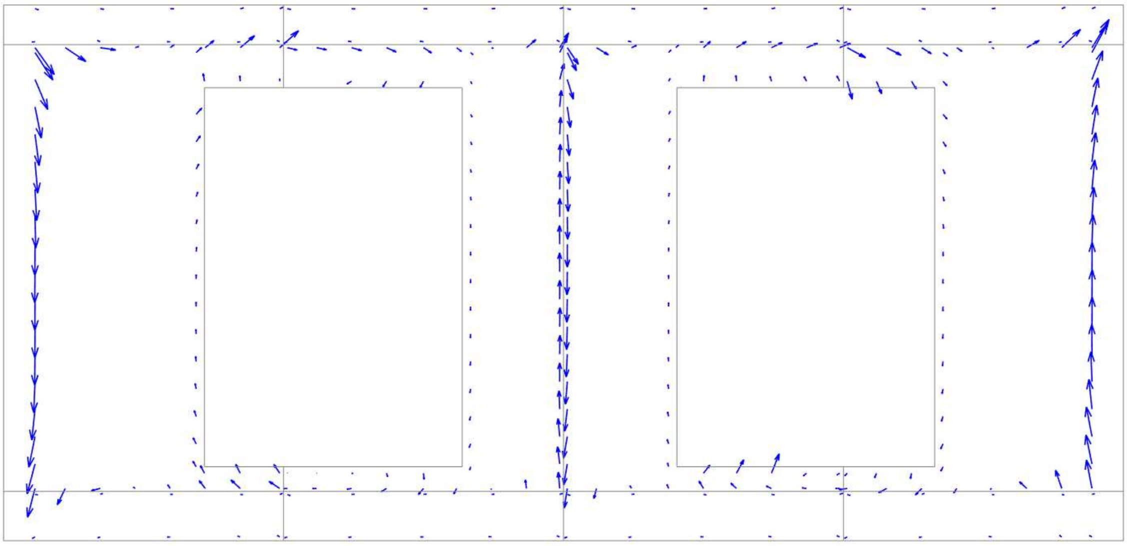

Figure 17. Screw DC displacement vector diagram at peak lateral load for FF-F&RW model.

The demand capacity (DC) ratio of the sheathing-to-CFS screw fasteners can be considered as an efficient indicator of their consumption. The DC ratio was defined as the ratio between the applied force on a given sheathing-to-CFS screw fastener and the peak capacity of the connection itself. The DC ratio for each screw in the shear wall at H/300 lateral drift (*i.e.*, elastic design threshold) is provided in Figure 18a, 19a and 20a for GF-FW, GF-RW, and FF-FW, respectively. At the H/300 displacement level, the response of the sheathing-to-CFS screws remains elastic and the maximum stress applied on the sheathing boards is below the allowable elastic values. This is in line with the linear elastic structural design philosophy. The values of the DC ratio of the screws in the vertical straight edges of the sheathing boards are relatively higher compared to the screws in the other parts of the wall, at all levels of lateral demand. At the peak load, several screws in the vertical edges of the sheathing boards have already been fully consumed (see Figures 18b, 19b and 20b). Furthermore, a smooth transition in the DC ratio in adjacent screws is witnessed in Figures 18a, 19a and 20a which indicates that significant redistribution of load among screws will take place if any screw was poorly or miss driven in the sheathing and/or the steel.

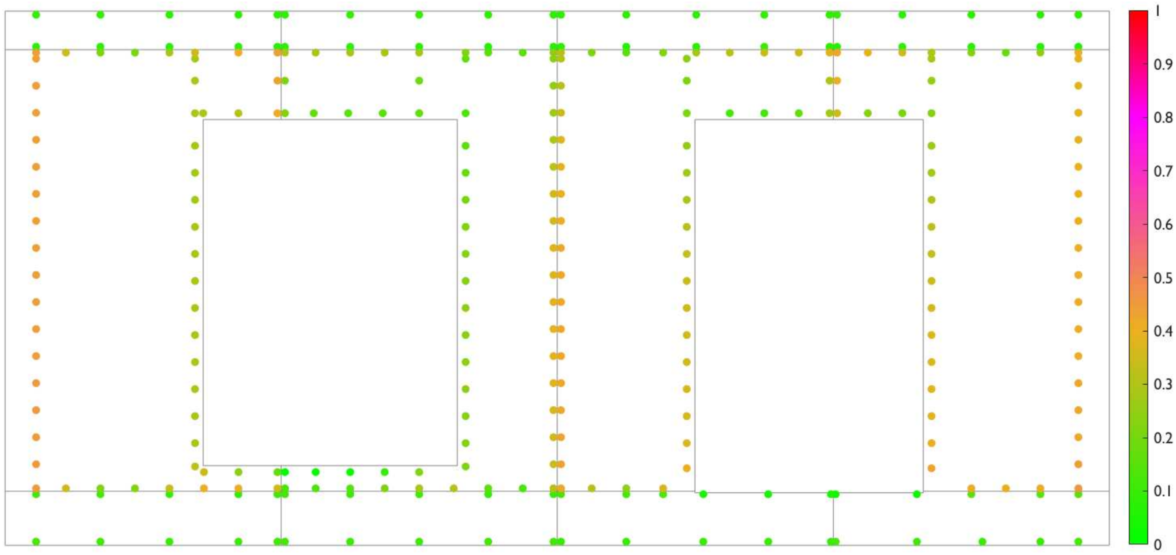

a)

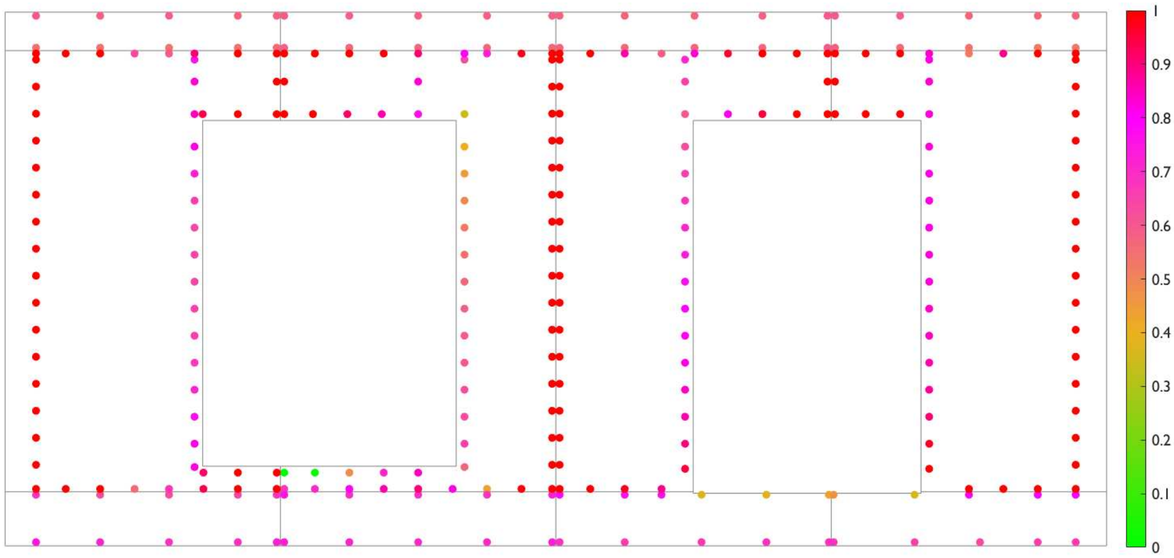

b)

Figure 18. Shear wall screw DC ratios in GF-FW: a) at H/300 lateral displacement and b) at peak lateral load.

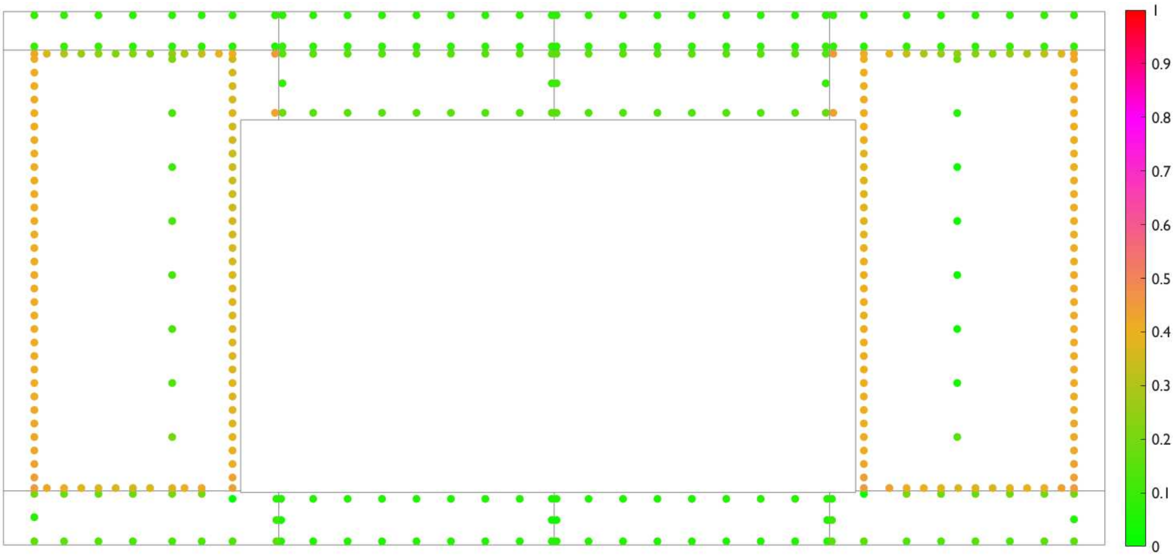

a)

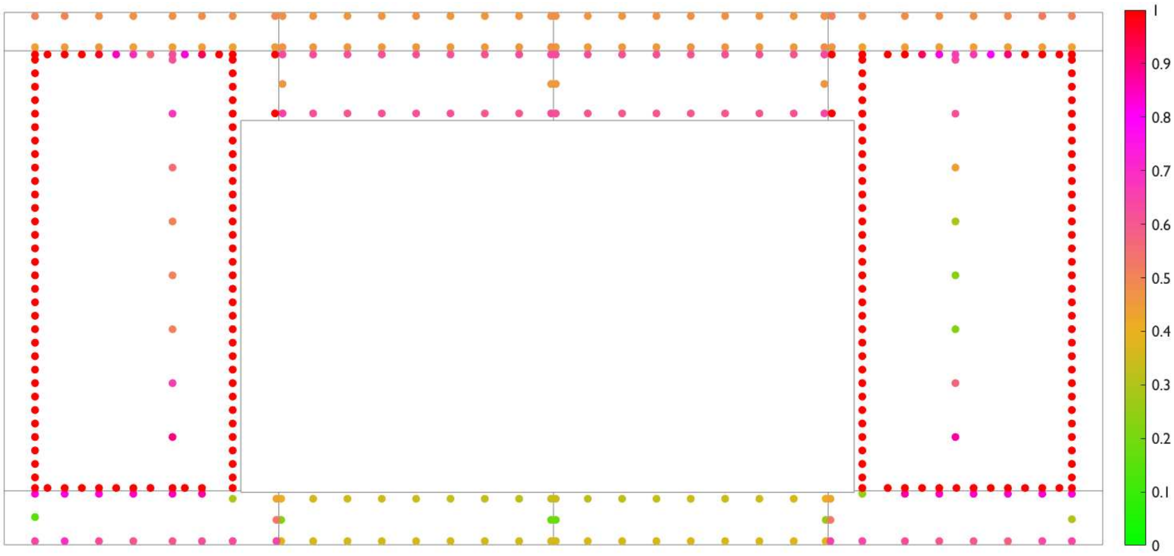

b)

Figure 19. Shear wall screw DC ratios in GF-RW: a) at H/300 lateral displacement and b) at peak lateral load.

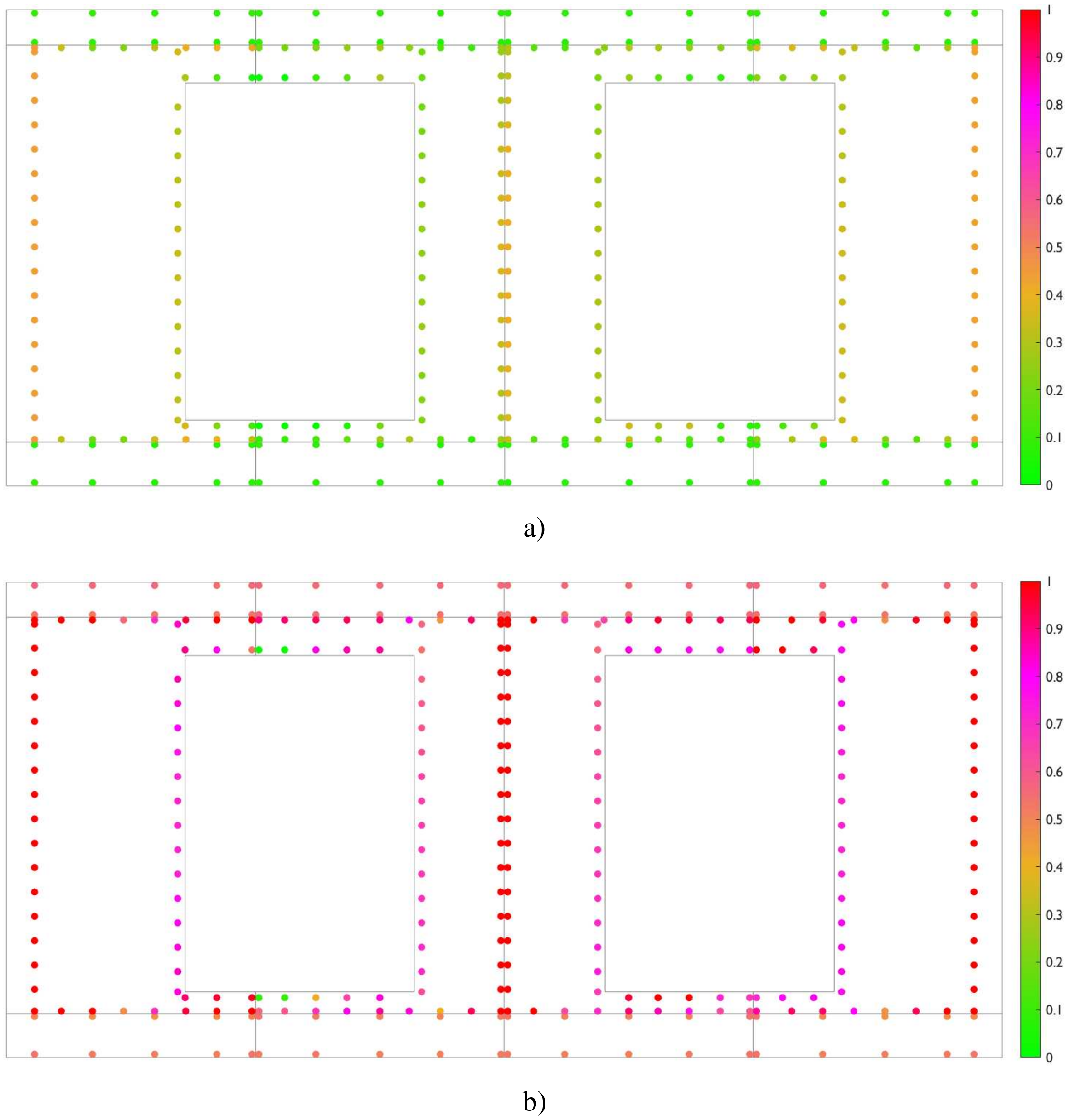

Figure 20. Shear wall screw DC ratios in FF-F&RW: a) at H/300 lateral displacement and b) at peak lateral load.

5. Results comparison with the perforated design methods

Currently, the North American Standard for Seismic Design of Cold-Formed Steel Structural Systems AISI S400-15 (2015) [42] is the main standard for the lateral design of CFS framed shear walls [34] that are labelled as either Type I or Type II. As stated in the AISI S400-15 document, "Type I shear wall is designed to resist in-plane lateral forces that is fully sheathed and that is provided with hold-downs and anchorage at each end of the wall segment. Type II shear wall is designed to resist in-plane lateral forces that is sheathed with wood structural panels or steel sheet sheathing that contains openings, but which has not been specifically designed and detailed for force transfer around openings. Hold-downs and anchorage for Type II shear walls are only required at the ends of the wall" [42]. Openings are accounted for by an empirical adjustment factor (see Equation 1) which is given as a function of maximum opening height ratio and percentage of full-height segment. It is worth mentioning that the contribution of the sheathing above and below openings is ignored in the determination of Type II shear wall lateral capacity as given in the following expression:

$$V_n = C_a v_n \sum L_i \tag{1}$$

Where C_a refers to the adjustment factor, v_n is the nominal shear strength per unit length, and $\sum L_i$ is the sum of the length of Type II shear wall segments [42].

A comparison of experimental test and FEA results is made and presented in Table 4 with estimates of strength using the Type II design approach that is currently outlined in the AISI S400-15 code for CFS shear wall with openings. The table shows that AISI equation gives conservative values of the shear strength. This can be explained as, in the AISI, merely the full-height segments are accounted for resisting the applied lateral loads which in turn resulted in not making use of the full wall geometry, thus, leading to a conservative lateral design.

Table 4. Comparison of experimental test and FEA results with AISI S-400-15 predictions of Type II shear wall lateral strength.

Wall configuration	**Shear strength (kN)**	**FEA (kN)**	**Ca (AISI S400-15)**	**$\sum L_i$ (mm)**	**v_n (AISI S400) (kN)**	**Vn (AISI S400) (kN)**	**FEA/ test**	**AISI/ test**
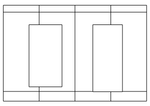	55.62	61.50	0.67	2413.9	9.90	16.01	1.11	0.29
	61.40						1.00	0.26
	61.61						1.00	0.26
Mean	**59.54**	**-**	**-**	**-**	**-**	**-**	**1.04**	**0.27**
STDEV	**2.78**	**-**	**-**	**-**	**-**	**-**	**0.05**	**0.01**
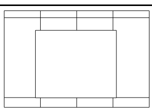	64.30	64.52	0.63	1861.4	18.50	21.69	1.00	0.34
	64.90						0.99	0.33
	58.00						1.11	0.37
Mean	**62.40**	**-**	**-**	**-**	**-**	**-**	**1.04**	**0.35**
STDEV	**3.12**	**-**	**-**	**-**	**-**	**-**	**0.05**	**0.02**
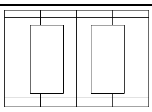	58.68	60.28	0.67	2301.4	9.90	15.27	1.03	0.26
	59.70						1.01	0.26
	60.14						1.00	0.25
Mean	**59.51**	**-**	**-**	**-**	**-**	**-**	**1.01**	**0.26**
STDEV	**0.61**	**-**	**-**	**-**	**-**	**-**	**0.01**	**0.00**

In addition to the AISI-based design approach, several researchers have developed equations for the perforated design method to gauge the impact of door and window apertures on the lateral strength of CFS framed shear walls. As per Sugiyama and Matsumoto (1994) [36], the ratio of the sheathing area is defined as:

$$\gamma = \frac{1}{1 + \frac{A_0}{H \sum L_i}} \tag{2}$$

In the above expression, A_0 refers to the total area of openings, H refers to the height of the wall, and $\sum L_i$ refers to the sum of the lengths of full-height segments.

As for the adjustment factor *i.e.*, the ratio of the lateral capacity of a shear wall with openings (as per the perforated design method) to the lateral capacity of a solid shear wall (without openings), it can be determined using the following expression:

$$F = \frac{\gamma}{3 - 2\gamma} \tag{3}$$

As part of the testing program undertaken at the National Association of Home Builders (NAHB) Research Center (1997) [35], Equation 2 was scrutinized and it turned out to be conservative and the following equation was suggested:

$$F = \frac{\gamma}{2 - \gamma} \tag{4}$$

Additionally, Yang J. (2011) [41] proposed the following exponential equation by compiling the results of previous tests carried out on CFS framed shear walls with openings:

$$F = \exp\left(1.128 - \frac{1.163}{\eta}\right) \tag{5}$$

Where η refers to the percentage of the area of the openings as defined in the following equation:

$$\eta = \frac{A - A_0}{A} \tag{6}$$

In Equation 6, A refers to the total area of the wall, and A_0 refers to the total area of openings within the wall.

A comparison of experimental test and FEA results with estimates of strength using the above-described approaches is made and presented in Table 5. Similar to what has been concluded from the comparison with the AISI-based approach, conservative values of the lateral capacity of CFS framed shear walls were obtained from Equations 3-5 as the parts of the shear wall above and below the openings are not accounted for.

Table 5. Comparison of experimental test and FEA results with Equations 3-5 predictions of shear wall lateral strength.

Wall configuration	Shear strength (kN)	FEA (kN)	γ	η	F3*	F4*	F5*	FEA/ test	F3/test	F4/test	F5/test
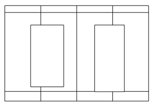	55.62	62.25	0.69	0.63	0.36	0.39	0.46	1.11	0.30	0.32	0.38
	61.40							1.00	0.27	0.29	0.34
	61.61							1.00	0.27	0.29	0.34
Mean	**59.54**	**-**	**-**	**-**	**-**	**-**	**-**	**1.04**	**0.28**	**0.30**	**0.35**
STDEV	**2.78**	**-**	**-**	**-**	**-**	**-**	**-**	**0.05**	**0.01**	**0.01**	**0.02**
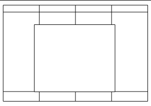	64.30	64.52	0.59	0.50	0.25	0.27	0.33	1.00	0.33	0.36	0.44
	64.90							0.99	0.32	0.35	0.43
	58.00							1.11	0.36	0.40	0.48
Mean	**62.40**	**-**	**-**	**-**	**-**	**-**	**-**	**1.04**	**0.34**	**0.37**	**0.45**
STDEV	**3.12**	**-**	**-**	**-**	**-**	**-**	**-**	**0.05**	**0.02**	**0.02**	**0.02**
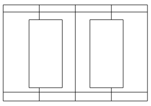	58.68	60.28	0.66	0.60	0.33	0.36	0.42	1.03	0.25	0.27	0.33
	59.70							1.01	0.25	0.27	0.32
	60.14							1.00	0.25	0.27	0.32
Mean	**59.51**	**-**	**-**	**-**	**-**	**-**	**-**	**1.01**	**0.25**	**0.27**	**0.32**
STDEV	**0.61**	**-**	**-**	**-**	**-**	**-**	**-**	**0.01**	**0.00**	**0.00**	**0.00**

**F3, F4, and F5 correspond to the adjustment factor obtained from Equations 3, 4 and 5, respectively.*

6. Summary and conclusions

This paper presented an investigation into the performance of CFS framed shear walls with openings under in-plane lateral loads. Overall, three shear wall typologies were designed according to the FTAO method then tested under monotonic lateral loads. A detailed FEA modelling protocol was elaborated to simulate the lateral behaviour of the tested walls as well as to gain insights into the force transfer around openings in CFS framed shear walls subjected to lateral loads. Subsequently, the output of load and displacement for each sheathing-to-CFS screw facilitated load-path mappings which in turn enabled the analysis of the flow of the in-plane lateral loads from the sheathing-to-CFS screw level into the wall system level. Eventually, a comparison of the experimental test and FEA results with that of the AISI S400-15 design provisions for Type II shear walls and that of the perforated design methods available in the literature was carried out.

Following are the major conclusions that were reached in this study:

- Comparison between numerical and experimental test results validated the developed FEA modelling protocol that turned out to be reliable in replicating the lateral behaviour of CFS framed shear walls with openings. Furthermore, the capability of the developed FEA modelling protocol to be used as a virtual test bench to improve and optimize the design of CFS framed shear walls was demonstrated.

- The numerical and experimental test results showed that the failure mode of CFS framed shear walls with openings, designed according to the FTAO method, is represented mainly by damages of the sheathing around the corners of the openings due to the force transfer around openings mechanism.
- C-shaped sheathing turned out to be an efficient detail for force transfer around openings where, depending on the applied forces, the need for strapping around openings could be dismissed.
- The FTAO method allows for a better lateral performance than the segmented and perforated design methods.
- A steady increase in the initial stiffness and peak strength is associated with the screw spacing reduction.
- The openings area ratio is inversely proportional to the initial stiffness and the peak strength of CFS framed shear walls. The geometry of sheathing panels influences the lateral behaviour of CFS shear walls especially if they were designed for force transfer around opening.
- Load-path mappings from the developed modelling protocol enabled the analysis of the flow of the in-plane lateral loads from sheathing-to-CFS screw level into the wall system level which helped in optimizing the screw density in the walls.

Outstanding matters regarding the lateral performance of CFS framed shear walls with openings include a possible investigation of the reinforcement of the corners of the openings as a detailing measure of force transfer around openings.

Acknowledgements

This research work has been developed under an Innovate UK supported Knowledge Transfer Partnership (KTP 11543) between the University of Leeds and a modular housing developer ilke Homes Ltd. Special thanks to Nigel Banks, Research and Development Director at ilke Homes Ltd., for his contribution throughout all stages of this study. The numerical simulations were undertaken on ARC4, part of the High-Performance Computing facilities at the University of Leeds, UK.

References

[1] EN 1993-1-1, Eurocode 3, Design of steel structures, Part 1.1: General rules and rules for buildings, European Committee for Standardization, Brussels, CEN, 2005.

[2] Kechidi S, Macedo L, Castro JM, Bourahla N. Seismic risk assessment of cold-formed steel shear wall systems. Journal of Constructional Steel Research 2017; 138: 565-579.

[3] EN 1993-1-3, Eurocode 3, Design of steel structures, Part 1.3: General rules for cold formed thin gauge members and sheeting, European Committee for Standardization, Brussels, CEN, 2006.

[4] EN 1993-1-5, Eurocode 3, Design of steel structures, Part 1.5: Plated structural elements, European Committee for Standardization, Brussels, CEN, 2019.

[5] EN 1993-1-8, Eurocode 3, Design of steel structures, Part 1.8: Design of joints, European Committee for Standardization, Brussels, CEN, 2005.

[6] Branston AE, Chen CY, Boudreault FA, and Rogers CA. Testing of light-gauge steel frame wood structural panel shear walls. Canadian Journal of Civil Engineering 2006; 33(9): 561-572.

[7] Serrette R, Nolan DP. Reversed cyclic performance of shear walls with wood panels attached to cold-formed steel with pins. Journal of Structural Engineering 2009; 135(8): 959-967.

[8] Landolfo R, Fiorino L, Corte DG. Seismic behavior of sheathed cold-formed structures: Physical tests. Journal of Structural Engineering 2006; 132(4): 570-581.

[9] Hikita K, Rogers CA. Impact of gravity loads on the lateral performance of light gauge steel frame/wood panel shear walls, Proceedings of the ninth Canadian Conference on Earthquake Engineering, Ottawa, Ontario, Canada 26-29 June 2007.

[10] DaBreo J, Balh N, Ong-Tone C, Rogers CA. Steel sheathed cold-formed steel framed shear walls subjected to lateral and gravity loading. Thin-Walled Structures 2014; 74: 232-245.

[11] Iuorio O, Fiorino L, Landolfo R. Testing CFS structures: The new school BFS in Naples. Thin-Walled Structures 2014; 84: 275-288.

[12] Selvaraj S, Madhavan M. Investigation on sheathing-fastener connection failures in cold-formed steel wall panels. Structures 2019; 20: 176-188.

[13] Selvaraj S, Madhavan M. Influence of sheathing-fastener connection stiffness on the design strength of cold-formed steel wall panels. Journal of Structural Engineering 2020; 146(10): 04020202.

[14] Selvaraj S, Madhavan M. Bracing effect of sheathing in point-symmetric cold-formed steel flexural members. Journal of Constructional Steel Research 2019; 157: 450-462.

[15] Selvaraj S, Madhavan M, Lau HH. Sheathing-fastener connection strength based design method for sheathed CFS point-symmetric wall frame studs. Structures 2021; 33: 1473-1494.

[16] Kyprianou C, Kyvelou P, Gardner L, Nethercot DA. Experimental study of sheathed cold-formed steel beam-columns. Thin-Walled Structures 2021; 166: 108044.

[17] Yu C. Shear resistance of cold-formed steel framed shear walls with 0.681 mm, 0.762 mm, and 0.838 mm steel sheet sheathing. Engineering Structures 2010; 32: 1522-1529.

[18] Yu C, Chen Y. Detailing recommendations for 1.83 m wide cold-formed steel shear walls with steel sheathing. Journal of Constructional Steel Research 2011; 67(7): 93-101.

[19] American Iron and Steel Institute (AISI), Standard for cold-formed steel framing-lateral design 2007 edition, AISI S213, Washington, D.C., USA, (2007).

[20] Iuorio O, Fiorino L, Macillo V, Terracciano MT, Landolfo R. The influence of the aspect ratio on the lateral response of sheathed cold formed steel walls. 21th International Specialty Conference on Cold-formed Steel Structures 2012; 739-753.

[21] Landolfo R, Iuorio O, Fiorino L. Experimental seismic performance evaluation of modular lightweight steel buildings within the ELISSA project. Earthquake Engineering and Structural Dynamics 2018; 47: 2921-2943.

[22] Martínez-Martínez JM, Xu L. Simplified nonlinear finite element analysis of buildings with CFS shear wall panels. Journal of Constructional Steel Research 2010: 67(12): 565-575.

[23] Shamim I. and Rogers CA. Steel sheathed/CFS framed shear walls under dynamic loading: Numerical modelling and calibration. Thin-Walled Structures 2013; 71: 57-71.

[24] Nithyadharan M, Kalyanaraman V. Modelling hysteretic behaviour of cold-formed steel wall panels. Thin-Walled Structures 2013; 46: 643-652.

[25] Buonopane SG, Bian G, Tun TH, Schafer BW. Computationally efficient fastener-based models of cold-formed steel shear walls with wood sheathing. Journal of Constructional Steel Research 2015; 110: 137-148.

[26] Ye J, Feng R, Chen W, Liu W. Behavior of cold-formed steel wall stud with sheathing subjected to compression. Journal of Constructional Steel Research 2016; 116: 79-91.

[27] Peterman KD, Schafer BW. Cold-formed steel studs under axial and lateral load. Journal of Structural Engineering 2014; 140(10): 04014074.

[28] Kechidi S, Bourahla N. Deteriorating hysteresis model for cold-formed steel shear wall panel based on its physical and mechanical characteristics. Thin-Walled Structures 2016; 98(Part B): 421-430.

[29] Kechidi S, Fratamico DC, Schafer BW, Castro JM, Bourahla N. Simulation of screw connected built-up cold-formed steel lipped channels under axial compression. Engineering Structures 2020; 206: 110109.

[30] Derveni F, Gerasimidis S, Peterman KD. Behavior of cold-formed steel shear walls sheathed with high-capacity sheathing. Engineering Structures 2020; 225: 111280.

[31] Derveni F, Gerasimidis S, Schafer BW, Peterman KD. High fidelity finite element modeling of wood-sheathed cold-formed steel shear walls. Journal of Structural Engineering 2021; 147: 04020316.

[32] Nithydharan M, Kalyanaraman V. A new screw connection model and FEA of CFS shear wall panels. Journal of Constructional Steel Research 2021; 176: 106430.

[33] Fiorino L, Iuorio O, Landolfo R. Sheathed cold-formed steel housing: A seismic design procedure. Thin-Walled Structures, 2009; 47, 919-930.

[34] Kechidi S, Bourahla N, Castro JM. Seismic design procedure for cold-formed steel sheathed shear wall frames: Proposal and evaluation. Journal of Constructional Steel Research 2017; 128: 219-232.

[35] National Association of Home Builders (NAHB) Research Center for the American Iron and Steel Institute. Monotonic tests of cold-formed steel shear walls with opening. 1997.

[36] Sugiyama H, Matsumoto T. Empirical equation the estimation of racking strength of a plywood-sheathed shear wall with openings. Summaries of Technical Papers of Annual Meeting Architectural Institute of Japan. Structures II, 1994.

[37] Salenikovich AJ, Dolan JD, Easterling WS. Racking performance of long steel-frame shear walls, International Specialty Conference on Cold-Formed Steel Structures, 2000.

[38] Dolan JD, Easterling WS. Monotonic and cyclic tests of light-frame shear walls with various aspect ratios and tie-down restraints. Blacksburg, VA, 2000.

[39] Dolan JD, Easterling WS. Effect of anchorage and sheathing configuration on the cyclic response of long steel-frame shear walls. Blacksburg, VA, 2000.

[40] Fülöp L, Dubina D. Performance of wall-stud cold-formed shear panels under monotonic and cyclic loading Part I: Experimental research. Thin-Walled Structures 2004; 42: 321-338.

[41] Yang J. Research on the shear resistance of cold-formed steel stud composite wall, Master thesis, Tongji University, 2006 (in Chinese).

[42] American Iron and Steel Institute (AISI), North American standard for seismic design of cold-formed steel structural systems, AISI S400, Washington, D.C., USA, 2015.

[43] Ornella Iuorio. Design procedures for cold formed steel housing in seismic area, PhD thesis, University of Naples "Federico II", Italy, 2009.

[44] Kyprianou C, Kyvelou P, Gardner L, Nethercot DA. Characterisation of material and connection behaviour in sheathed cold-formed steel wall systems – Part 1: Experimentation and data compilation. Structures 2021, 30: 1161-1183.

[45] BS EN 12369-1 (2001). Wood-based panels. Characteristic values for structural design. OSB, particleboards and fireboards, London, BSI.

[46] BS EN ISO 6892-1 (2019). Metallic materials. Tensile testing. Method of test at room temperature, London, BSI.

[47] Kechidi S, Iuorio O. Numerical investigation into the effect of modular construction details on the lateral behaviour of cold-formed steel framed shear walls. Engineering Structures 2022 (under review after a minor revision).

[48] BS EN 594 (1996). Timber structures - Test methods - Racking strength and stiffness of timber frame wall panels, London, BSI.

[49] ABAQUS (2017). "Abaqus theory guide." *Version 2017*, Dassault Systems Simulia Corp., United States.

[50] Constantinos Kyprianou. Sheathed cold-formed steel wall systems, PhD thesis, Imperial College London, United Kingdom, 2021.

[51] https://mdfosb.com/en/products/smartply-max. Accessed 03/11/2021.

[52] https://www.buildingboards.co.uk/products/rcm-multipurpose/. Accessed 03/11/2021.

[53] Lowes LN, Altoontash A. Modeling the Response of Reinforced Concrete Beam-Column Joints. Journal of Structural Engineering 2003; 129: 1686-1697.

[54] PEER, OpenSees: Open system for earthquake engineering simulation, Pacific Earthquake Engineering Research Center, University of California, Berkeley, CA, 2006.

[55] Ding C. Monotonic and cyclic simulation of screw-fastened connections for cold-formed steel framing, MSc. thesis, Virginia Tech, Blacksburg, VA, United States, 2015.